

Multilevel sensitization of Er³⁺ in low-temperature-annealed silicon-rich SiO₂

Oleksandr Savchyn,^{1,a)} Ravi M. Todi,² Kevin R. Coffey,^{2,b)} and Pieter G. Kik^{1,b)}

¹CREOL, The College of Optics and Photonics, University of Central Florida, 4000 Central Florida Blvd., Orlando, Florida 32816, USA

²Advanced Materials Processing and Analysis Center (AMPAC), University of Central Florida, 4000 Central Florida Blvd., Orlando, Florida 32816, USA

(Received 31 October 2008; accepted 18 November 2008; published online 12 December 2008)

The dynamics of Er³⁺ excitation in low-temperature-annealed Si-rich SiO₂ are studied. It is demonstrated that Si-excess-related indirect excitation is fast (transfer time $\tau_{tr} < 27$ ns) and occurs into higher lying Er³⁺ levels as well as directly into the first excited state (⁴I_{13/2}). By monitoring the time-dependent Er³⁺ emission at 1535 nm, the multilevel nature of the Er³⁺ sensitization is shown to result in two types of excitation of the ⁴I_{13/2} state: a fast excitation process ($\tau_{tr} < 27$ ns) directly into the ⁴I_{13/2} level and a slow excitation process due to fast excitation into Er³⁺ levels above the ⁴I_{13/2} level, followed by internal Er³⁺ relaxation with a time constant $\tau_{32} > 2.3$ μ s. The fast and slow excitations of the ⁴I_{13/2} level account for an approximately equal fraction of the excitation events: 45%–50% and 50%–55%, respectively. © 2008 American Institute of Physics.

[DOI: 10.1063/1.3044480]

The continued technological implementation of Si photonics requires the development of a cost effective Si-compatible light source.^{1–4} The use of Si nanocrystals (NCs) as sensitizers of Er³⁺ ions⁵ and the subsequent demonstration of Si-sensitized gain at 1.54 μ m (Ref. 6) have drawn significant attention since this approach could potentially enable the realization of an on-chip laser under excitation with a low-cost broadband light source. Despite significant promise of this approach, the presence of Si NCs was found to result in a low concentration of optically active erbium ions^{7,8} and to introduce significant confined carrier absorption^{9–11} as well as scattering.¹² Recently it has been shown that broadband sensitization of Er³⁺ can also occur in Si-doped SiO₂ annealed at temperatures well below those required for NC formation.^{7,8,13} This phenomenon has been attributed to Er³⁺ excitation by Si-excess-related luminescence centers (LCs) in the SiO₂ matrix.^{7,8} Such low-temperature-annealed samples were found to contain a higher density of optically active Er³⁺ ions compared to Si-NC-doped samples with similar total Si and Er concentrations.^{7,8} In addition, the absence of Si NCs in low-temperature annealed samples could minimize scattering as well as confined carrier absorption typically introduced by Si NCs during optical pumping.^{9,10} These factors make low-temperature-annealed Er-doped Si-rich SiO₂ an interesting candidate for the realization of amplification at 1.54 μ m under broadband excitation. The evaluation of this material as a gain medium requires a detailed understanding of the observed Er³⁺ excitation process. The present study discusses the dynamics of the LC-mediated Er³⁺ excitation mechanism in low-temperature-annealed Er-doped Si-rich SiO₂.

An Er-doped Si-rich SiO₂ film (thickness 110 nm) containing 12 at. % of excess Si and 0.63 at. % of Er was deposited by magnetron cosputtering onto a Si wafer. The sample was annealed for 100 s in N₂ at 600 °C and subse-

quently passivated for 30 min in forming gas (N₂:H₂ = 95%:5%) at 500 °C. No Si aggregates could be detected in transmission electron microscopy measurements on this sample.⁷ For optical measurements, the sample was attached to the cold finger of a closed-loop He cryostat (ARS, DE-202 AET) and held at 15 K at a pressure of 5×10^{-7} mbar. Photoluminescence (PL) spectra were taken using the 351 nm line of a Kr-ion laser as the excitation source (0.26 W/cm²). PL spectra in the regions of 500–1100 and 950–1750 nm were recorded using a charge-coupled device array and a Ge detector respectively, with a spectral resolution of 10 nm. The PL spectra were corrected for the system spectral response and concatenated at $\lambda = 1025$ nm. The time-dependent PL signal was measured under pulsed excitation using the 355 nm line of a Nd:YAG (neodymium doped yttrium aluminum garnet) laser (Spectra Physics, Quanta Ray GCR-150-30). The full width at half maximum pulse length Δt , the pulse energy, the repetition rate, and the $1/e^2$ spot size were 5 ns, 1.9 μ J, 30 Hz, and 1.9 mm², respectively. PL decay traces at emission wavelengths of 981 and 1535 nm were obtained using a photomultiplier tube. Unless otherwise stated, the PL decay traces were recorded with a time resolution of 80 ns. The maximum time resolution in the PL decay measurements was ~ 27 ns, most likely due to pulse timing jitter. In all measurements, the sample was scanned to minimize the possibility of light-induced changes to the optical properties of the sample upon exposure to UV light.¹⁴ Further details on the experimental procedures can be found in Refs. 7 and 8.

Figure 1 shows the PL spectrum in the region of 500–1700 nm. The spectrum shows four emission bands: a broad emission band peaking around ~ 600 nm corresponding to the emission from Si-excess-related LCs in the Si-rich SiO₂ matrix,^{15,16} two narrow bands peaking at 981 and 1535 nm corresponding to the transition from, respectively, the second (⁴I_{11/2}) and first (⁴I_{13/2}) excited states of the Er³⁺ ions to the ground state (⁴I_{15/2}), and a weak emission peak at 1128 nm, most likely due to radiative exciton recombination in the Si

^{a)}Electronic mail: osavchyn@mail.ucf.edu.

^{b)}Also at the Physics Department, University of Central Florida.

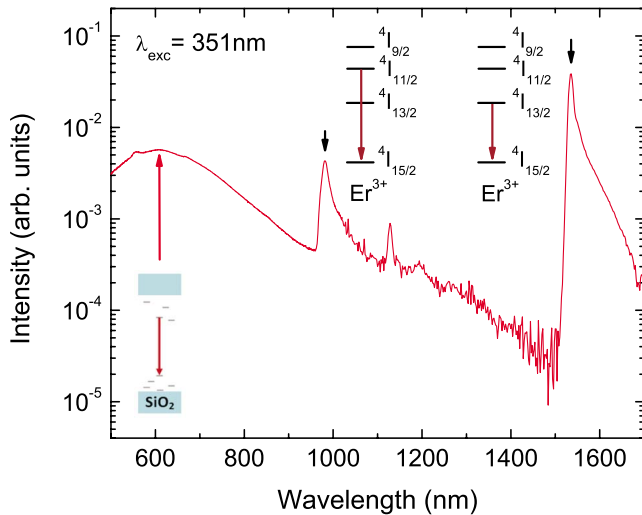


FIG. 1. (Color online) PL spectrum of low-temperature-annealed Er-doped Si-rich SiO_2 measured at 15 K. Emission from LC and Er^{3+} ions is indicated schematically on energy diagrams.

substrate. At this pump power, no Er-related PL signal could be detected during either continuous wave (cw) excitation or pulsed excitation from a reference sample containing a similar concentration of Er (0.49 at. %) but no excess Si. This demonstrates that the observed Er^{3+} emission is predominantly excited indirectly via a Si-excess-related mechanism. Power-dependent cw and pulsed PL measurements (not shown) indicated that second order processes such as cooperative upconversion and excited state absorption do not significantly contribute to the observed 981 nm emission in these experiments.

Figure 2 shows the PL decay trace detected at 981 nm under pulsed excitation. The signal shows a sharp initial peak followed by a much slower multiexponential decay. The decay after the initial peak was fitted with a stretched exponential function of the form $I_3(t) = I_3(0) \exp[-(t/\tau_3)^{\beta_3}]$, with a decay time $\tau_3 = 2.38 \pm 0.07 \mu\text{s}$ and dispersion factor β_3

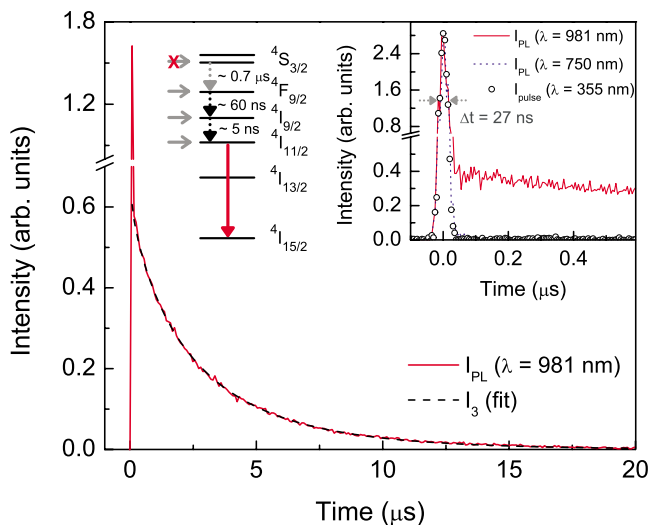


FIG. 2. (Color online) Time-dependent PL intensity at 981 nm under pulsed excitation (I_{PL} , solid line) with the corresponding fit (I_3 , dashed line). The Er^{3+} level diagram indicates possible excitation pathways and typical multiphonon relaxation times. Inset: Er^{3+} emission at 981 nm (I_{PL} , solid line), the LC emission at 750 nm (I_{PL} , dotted line), and the pump pulse (I_{pulse} , open circles) scaled to the same maximum value.

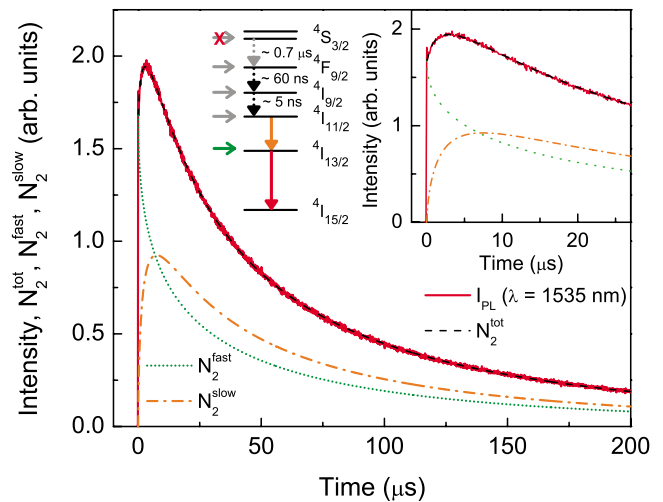


FIG. 3. (Color online) Time-dependent PL intensity at 1535 nm under pulsed excitation (I_{PL} , solid line) with the corresponding fit (N_2^{tot} , dashed line), including the individual time-dependent contributions due to excitation by the fast (N_2^{fast}) and slow (N_2^{slow}) mechanisms. The Er^{3+} level diagram indicates possible excitation pathways. The inset shows the same data in the range of 0–27 μs .

$= 0.79 \pm 0.01$ (dashed line). The inset of Fig. 2 shows the same signal measured with a detection resolution of 5 ns as well as the laser pulse shape (open circles, $\Delta t \approx 27$ ns) and the LC emission at 750 nm (dotted line) scaled to the same peak value. The LC emission can be seen to have a lifetime of < 27 ns. The initial peak detected at 981 nm exhibits the same jitter-limited length of 27 ns, and is attributed to background emission from LCs at 981 nm (see Fig. 1). At this same wavelength, scattered laser light was estimated to contribute less than $\sim 2\%$ to the total signal.

The absence of a resolvable Er^{3+} signal rise after the excitation pulse in Fig. 2 demonstrates that the energy transfer time of the fast excitation process of Er^{3+} into the second excited state τ_{tr} is shorter than ~ 27 ns. Based on this observation, possible excitation channels leading to the 981 nm emission include excitation by LCs directly into the Er^{3+} $^4I_{11/2}$ level, or excitation into higher lying Er^{3+} levels followed by internal relaxation of the Er^{3+} ion on a time scale of < 27 ns. The Er^{3+} energy level diagram in Fig. 2 lists typical room-temperature nonradiative relaxation times for Er^{3+} in glass hosts.¹⁷ Taking into account the predominantly multiphonon nature of the relaxation, the relaxation times at 15 K are expected to be longer than the listed values.¹⁸ Of the shown relaxation paths, only the $^4S_{3/2} \rightarrow ^4F_{9/2}$ relaxation is significantly slower than 27 ns. We therefore conclude that the most likely excitation paths of the 981 nm emission are LC-mediated excitation either directly into the $^4I_{11/2}$ level or into the $^4I_{9/2}$ or $^4F_{9/2}$ levels followed by rapid relaxation to the $^4I_{11/2}$ level.

Figure 3 shows the PL decay trace taken at 1535 nm. The signal shows a fast rise followed by a slow decay. The inset of Fig. 3 shows the signal in the first 27 μs after excitation. Two different excitation processes can be distinguished: fast excitation (< 27 ns) resulting in the rise of the signal up to $\sim 80\%$ of its maximum value and slow excitation taking place on the time scale of ~ 2 – $3 \mu\text{s}$. Reference measurements taken at wavelengths in the range of 1200–1500 nm (not shown) revealed only the resolution-limited initial peak but no slow rise and decay. This demonstrates

that all emission at 1535 nm observed after the initial peak is due to Er^{3+} emission from the first excited state. The similarity between the decay time of the second excited state ($\sim 2.38 \mu\text{s}$) and the duration of the slow excitation of the first excited state ($\sim 2-3 \mu\text{s}$) suggests that the slow excitation results from internal relaxation of the Er^{3+} ion from the ${}^4I_{11/2}$ to the ${}^4I_{13/2}$ level.

Based on the experimental observations, it appears that the time-dependent emission from the first excited state [and thus its total population $N_2^{\text{tot}}(t)$] contains the two following contributions: emission from Er^{3+} ions excited into the first excited state via a fast excitation mechanism (N_2^{fast}) and emission from Er^{3+} ions excited via a slow excitation mechanism (N_2^{slow}) due to the relaxation of Er^{3+} ions from the second excited state (characterized by the population N_3) to the first excited state. The time-dependent populations are described by the following rate equations:

$$\begin{aligned} \frac{dN_3(t)}{dt} &= -\frac{N_3(t)}{\tau_3}, \\ \frac{dN_2^{\text{slow}}(t)}{dt} &= \frac{N_3(t)}{\tau_{32}} - \frac{N_2^{\text{slow}}(t)}{\tau_2}, \\ \frac{dN_2^{\text{fast}}(t)}{dt} &= -\frac{N_2^{\text{fast}}(t)}{\tau_2}, \end{aligned} \quad (1)$$

where τ_2 is the decay time of the first excited state and τ_{32} is the relaxation time from the second to the first excited state. These equations lead to the following time-dependent total intensity I_2^{tot} of the ${}^4I_{13/2} \rightarrow {}^4I_{15/2}$ transition:

$$I_2^{\text{tot}} \propto N_2^{\text{fast}}(0)e^{-(t/\tau_2)\beta_2} + \frac{N_3(0)}{\tau_{32}(\tau_3^{-1} - \tau_2^{-1})} [e^{-(t/\tau_2)\beta_2} - e^{-(t/\tau_3)\beta_3}], \quad (2)$$

where the dispersion factors β_2 and β_3 have been added to account for the multiexponentiality of the decay. Setting both dispersion factors to 1 reduces Eq. (2) to the analytical solution of Eq. (1). Fitting the trace measured at 1535 nm with Eq. (2) yields the following parameter values: $\tau_2 = 20.7 \pm 1.9 \mu\text{s}$, $N_3(0)/[\tau_{32}N_2^{\text{fast}}(0)] = (4.93 \pm 0.52) \times 10^5 \text{ s}^{-1}$, $\tau_3 = 2.33 \pm 0.05 \mu\text{s}$, $\beta_2 = 0.49 \pm 0.01$, and $\beta_3 = 0.63 \pm 0.02$. The corresponding fit to the experimental trace and the respective time-dependent contributions to the population of the first excited state N_2^{fast} and N_2^{slow} are included in Fig. 3. The decay time $\tau_3 = 2.33 \mu\text{s}$ found from this fit and the value $\tau_3 = 2.38 \mu\text{s}$ found independently in Fig. 2 are equal within the experimental error. This observation provides strong support for the attribution of the slow excitation process to internal ${}^4I_{11/2} \rightarrow {}^4I_{13/2}$ relaxation and not to a slow LC-mediated excitation process. Taking into account that $\tau_3^{-1} = \tau_{31}^{-1} + \tau_{32}^{-1}$, with τ_{31}^{-1} the relaxation rate from level ${}^4I_{11/2}$ to the ground state, we find that the relaxation time τ_{32} is longer than $2.3 \mu\text{s}$. Time integration of the functions N_2^{fast} and N_2^{slow} yields a quantity proportional to the number of Er^{3+} ions

excited into the first excited state via the two excitation mechanisms. Performing this integration shows that $\sim 45\% - 50\%$ of the optically active sensitized Er^{3+} ions are excited directly into the ${}^4I_{13/2}$ level by LCs, while $\sim 50\% - 55\%$ are excited into the ${}^4I_{13/2}$ after LC-mediated excitation of the ${}^4I_{11/2}$ level followed by internal relaxation of the Er^{3+} ions. The presence of a large contribution of excitation via the ${}^4I_{11/2}$ level implies that the interlevel relaxation rate τ_{32}^{-1} will have a significant effect on the maximum net LC-mediated excitation rate of the ${}^4I_{13/2}$ level.

In summary, the mechanism of Er^{3+} excitation in low-temperature-annealed Er-doped Si-rich SiO_2 was studied. Er^{3+} excitation by LC was shown to occur directly into the ${}^4I_{13/2}$ level, as well as into higher lying levels, with a typical time constant of $< 27 \text{ ns}$. The presence of such a multilevel sensitization results in two types of excitation of the ${}^4I_{13/2}$ level of Er^{3+} : fast direct excitation ($\tau_{\text{tr}} < 27 \text{ ns}$) by the LCs and slow excitation due to the fast excitation of Er^{3+} ions into the higher energy levels with subsequent relaxation to the first excited state with a time constant $\tau_{32} > 2.3 \mu\text{s}$. It is shown that an approximately equal percentage of Er^{3+} ions are excited into the ${}^4I_{13/2}$ level by the fast (45%–50%) and slow (50%–55%) processes.

This work was supported by the National Science Foundation Career No. ECCS-0644228. We are grateful to Dr. R. E. Peale for providing us with access to the Nd:YAG laser used in these studies.

¹M. Lipson, *J. Lightwave Technol.* **23**, 4222 (2005).

²T. J. Kippenberg, J. Kalkman, A. Polman, and K. J. Vahala, *Phys. Rev. A* **74**, 051802 (2006).

³Q. Lin, T. J. Johnson, R. Perahia, C. P. Michael, and O. J. Painter, *Opt. Express* **16**, 10596 (2008).

⁴M. Makarova, V. Sih, J. Warga, R. Li, L. Dal Negro, and J. Vuckovic, *Appl. Phys. Lett.* **92**, 161107 (2008).

⁵M. Fujii, M. Yoshida, Y. Kanzawa, S. Hayashi, and K. Yamamoto, *Appl. Phys. Lett.* **71**, 1198 (1997).

⁶H.-S. Han, S.-Y. Seo, and J. H. Shin, *Appl. Phys. Lett.* **79**, 4568 (2001).

⁷O. Savchyn, F. R. Ruhge, P. G. Kik, R. M. Todi, K. R. Coffey, H. Nukala, and H. Heinrich, *Phys. Rev. B* **76**, 195419 (2007).

⁸O. Savchyn, P. G. Kik, R. M. Todi, and K. R. Coffey, *Phys. Rev. B* **77**, 205438 (2008).

⁹P. G. Kik and A. Polman, *J. Appl. Phys.* **91**, 534 (2002).

¹⁰R. D. Kekatpure and M. L. Brongersma, *Nano Lett.* **8**, 3787 (2008).

¹¹D. Navarro-Urrios, A. Pitanti, N. Daldosso, F. Gourbilleau, R. Rizk, G. Pucker, and L. Pavesi, *Appl. Phys. Lett.* **92**, 051101 (2008).

¹²R. D. Kekatpure and M. L. Brongersma, *Phys. Rev. A* **78**, 023829 (2008).

¹³G. Franzó, S. Boninelli, D. Pacifici, F. Priolo, F. Iacona, and C. Bongiorno, *Appl. Phys. Lett.* **82**, 3871 (2003).

¹⁴S. Godefroo, M. Hayne, M. Jivanescu, A. Stesmans, M. Zacharias, O. I. Lebedev, G. Van Tendeloo, and V. V. Moshchalkov, *Nat. Nanotechnol.* **3**, 174 (2008).

¹⁵M. Zhu, Y. Han, R. B. Wehrspohn, C. Godet, and R. Etemadi, *J. Appl. Phys.* **83**, 5386 (1998).

¹⁶A. J. Kenyon, P. F. Trwoga, C. W. Pitt, and G. Rehm, *J. Appl. Phys.* **79**, 9291 (1996).

¹⁷E. Desurvire, C. R. Giles, and J. R. Simpson, *J. Lightwave Technol.* **7**, 2095 (1989).

¹⁸C. B. Layne, W. H. Lowdermilk, and M. J. Weber, *Phys. Rev. B* **16**, 10 (1977).